CFD Simulation on Supercritical Fluid Extraction of Black Pepper's Bioactive Compounds: Single Particle Study

Then Siew Ping,[*] Freddie Panau and Yudi Samyudia

Department of Chemical Engineering, School of Engineering, Curtin University, Sarawak Campus CDT 250, 98000 Miri, Sarawak, Malaysia

[*]Corresponding author: then.siewping@gmail.com

Abstract: *To gain a better understanding on the application of computational fluid dynamics (CFD) towards extraction using supercritical fluid, a single particle study was carried out. The flow behaviour of an ambient supercritical carbon dioxide flowing through a heated black pepper particle in vertical direction was studied. The transfer of heat from the heated particle to supercritical fluid was examined. Various groups of parameters in the following ranges were carried out for the simulations: pressure 3000 psi, 4000 psi and 5000 psi; temperature 4°C, 50°C and 55°C; and solvent flow rate 5 ml min^{-1}, 7.5 ml min^{-1} and 10 ml min^{-1}. The contour of velocity magnitude and streamline of the flow along the particle were presented. Temperature profile and the local heat flux value on the heated particle surface were captured. The drag coefficients and average Nusselt numbers obtained from the simulations had shown a good agreement with the numerical correlations from literature.*

Keywords: Supercritical fluid extraction, heat transfer, Nusselt number, drag coefficient, single spherical particle

1.   INTRODUCTION

The pharmaceutical value of black pepper's essential oil in enhancing drugs' bioavailability has increased the intention of the industry to develop black pepper extraction.[1] Supercritical fluid extraction (SFE) appears to be the most promising alternative over the conventional processes as supercritical fluid preserves the extract from solvent-contamination and thermal degradation.[2,3,4] Yet, the commercial applications of the SFE technology remain limited to a few high-value products due to high capital investment, and its novelty and complex operating system.[2] To adopt SFE to black pepper oil production line, optimum design of the process for guaranteed production yield is therefore essential. The details of the complex flow and the transfer phenomenon within the fixed bed need to be comprehensively studied and understood.

The objective to apply Computational Fluid Dynamics (CFD) in the study of particle bed extraction is to visualise the complex interactions between

flow, heat transfer, diffusion and reaction towards the changes of operating parameters in order to optimise the process and also to improve the empirical correlation of transport parameters that has been used for many years, but which has not yet yielded a satisfactory results. Constructing a correct particle bed which well defines the experimental set-up involves many difficulties such as contact points, meshes and the role of boundary layer. A single particle studies is therefore carried out to gain a better understanding on the application of CFD towards extraction using supercritical fluid.

In this paper, the flow behaviour of a supercritical fluid flowing through a single spherical particle and heat transfer between the particle and flowing supercritical fluid are studied. The interactions between flow and heat transfer towards the changes of operating parameters are investigated. The simulation results are validated by comparing with the literature correlations.

2.   EXPERIMENTAL

2.1   Geometry and Boundary Conditions

In order to attain the objectives above, a supercritical carbon dioxide with lower temperature flows through a 1 mm diameter black pepper particle which has higher temperature was simulated in Ansys Workbench version 14.5. The black pepper particle was defined as an isothermal static solid sphere. It was simulated in a cylindrical domain which has open boundary conditions as shown in Figure 1. The domain size is denoted by a × b × c where the dimensions are in multiples of particle diameter. Domain independent study was carried out to ensure that the cylindrical domain is "infinite" to the fluid flow through the solid particle and also to determine the appropriate domain sizes to be applied to all set-ups. The walls are set as moving wall which moves at the same velocity as the inlet flow, with a no slip boundary conditions imposed on them. The supercritical fluid was entering the domain with uniform velocity and at room temperature. A pressure outlet boundary was used and the gauge pressure was set to zero so that the absolute pressure will be equal to the operating pressure.
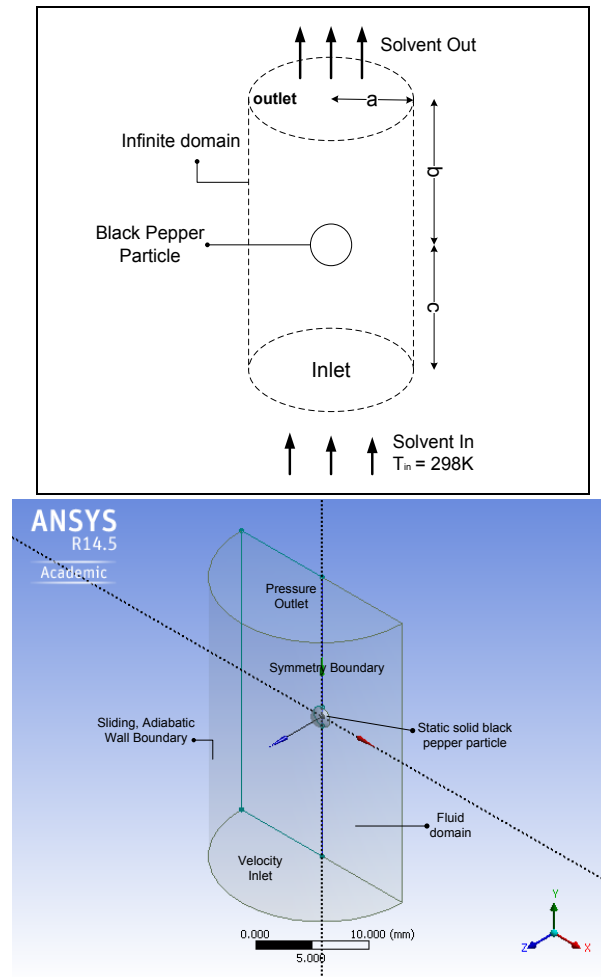
Figure 1:   Vertical flow through a single black pepper particle and asymmetrical 3D model developed in Ansys Workbench.

2.2   Materials and Parameters

A black pepper particle with 1 mm diameter was used for the simulations and carbon dioxide was used as the cycling fluid. The black pepper was defined as a solid body with constant properties of: density (1230 kg m^{-3}), heat capacity (2906 J kg^{-1} K^{-1}) and thermal conductivity (44 W m^{-1} K^{-1}). The density of black pepper was determined experimentally by using pycnometer while the heat capacity and thermal conductivity was obtained from the correlation derived by Meghwal.[5] The density of CO_2 was defined by using the fluent-built-in Peng-Robinson correlation and a piecewise polynomial correlation defined in Yaws[6]

was applied for heat capacity. Meanwhile, the correlation defined by Fenghour[7] was used for viscosity and a constant value of heat conductivity (0.0145 W m^{-1} K^{-1}) was considered during the simulations. Various groups of parameters in the following ranges was carried out for the simulations: pressure 3000 psi, 4000 psi and 5000 psi; temperature 45°C, 50°C and 55°C; and solvent flow rates of 5 ml min^{-1}, 7.5 ml min^{-1} and 10 ml min^{-1}.

2.3   Meshing

The precision of the simulation results depends on the size of the mesh around the hot spherical particle. A fine uniform mesh gives an accurate results yet it significantly increase the mesh size and thus increase the computational time. Therefore, the "Advanced Size Function" approach was used to control the transition from small prism cells on the on the sphere surface to a larger unstructured mesh of tetrahedral cells in the non-critical regions of the domain. This would significantly reduce the cells number and yet yield precise results. For solutions that were sufficiently grid independent, up to 4.7×10^4 mesh cells were required, with the first layer of cells thickness of 8.35×10^3 times the sphere diameter. The curvature size function was chosen and the curvature normal angle was set to 15° and growth rate was set to 1.2.

2.4   Computational Procedure

Pressure-based steady state simulations were performed for all cases. Converge was monitored by continuity, x-velocity, y-velocity and z-velocity equations, as well as the drag coefficient and the particle Nusselt number with the absolute criteria of 1e-6. The "SIMPLE" scheme solution method was used for pressure-velocity coupling. Second order upwind interpolation was applied to solve the Momentum and Energy equations. Least squares cell based was used for gradient and Standard was used for pressure. The Under-relaxation factors were left at the Fluent[TM] default values.

2.5   Validation

The heat transfer results were validated by comparing the dimensionless Nu to the empirical heat transfer relations by Ranz and Marshall,[8] Whitaker,[9] Achenbach[10] and Feng and etc.[11] for a single free sphere. The area-average Nu over the surface of the sphere was taken for comparison. The Nu of each cell on the particle surface was determined based on the local heat flux and temperature difference. The hydraulic length and reference temperature need to be correctly defined in order to get a precise value. The flow patterns were validated through the comparison of drag coefficients (C_D) with the correlation by Feng et al.,[11] Clift et al.[12] and Haider.[13] The drag coefficient of the simulation is readily

available in post-processing stage. The direction of drag force was defined to be the same as the flow of inlet fluid, and since asymmetry geometry was used, half of the total surface area is taken as the effective area to be used in calculating drag coefficient in the simulation.

3. RESULTS AND DISCUSSION

3.1 Domain-independence

The flow system defined was an isolated sphere in a flow of infinite domain, and since this must be computed in a finite domain, it is necessary to establish that the results are independent of the domain size. Domain independent studies were carried out and the results were tabulated in Table 1. The values of C_D and Nu were used to justify the domain independency. The domain sizes were determined by referring to the findings of Dixon.[14]

It was noticed that when a relatively small domain size was used, the value of C_D and Nu were dropped below the acceptable value. The domain size was therefore doubled up. When larger domain sizes were used, it was found that the changes in domain size had resulted in the difference below 8% in C_D and below 1% in Nu. This was thought to demonstrate domain independence to a satisfactory degree and a domain of $10 \times 5 \times 20$ was used for the simulations.

Table 1: The results of domain-independent tests.

Domain size $a \times c \times b$	C_D	Nu
$10 \times 5 \times 20$	0.44	40.76
$10 \times 5 \times 30$	0.41	41.144
$10 \times 10 \times 30$	0.42	40.12
$5 \times 10 \times 10$	0.348	38.90
$10 \times 5 \times 10$	0.29	42.079

3.2 Flow Pattern

The flow pattern of supercritical CO_2 flow through a heated solid sphere in vertical direction is as shown in Figure 2. In general, all cases of simulation condition give a similar fluid flow pattern, where the fluid velocity is brought to rest at the forward stagnation point and increase with the increase of stagnation angle. A formation of ring eddy attached to the rear surface of the sphere is noticed after the separation angle. The ring eddy is drawn out in the downstream direction and decayed as another forms. Turbulence wake is formed behind the

sphere. The length of the recirculation ring eddy region become pronounced when temperature and pressure of the sphere increases. It is expected that this recirculation would facilitate the heat transfer process. The angle of separation happens at 130° for the case of 3000 psi, 318K, 0.117 m s^{-1} and slightly increases when temperature, pressure and flow rate increase. The increases in temperature and pressure have also led to a higher velocity gradient on the surface of the particle.
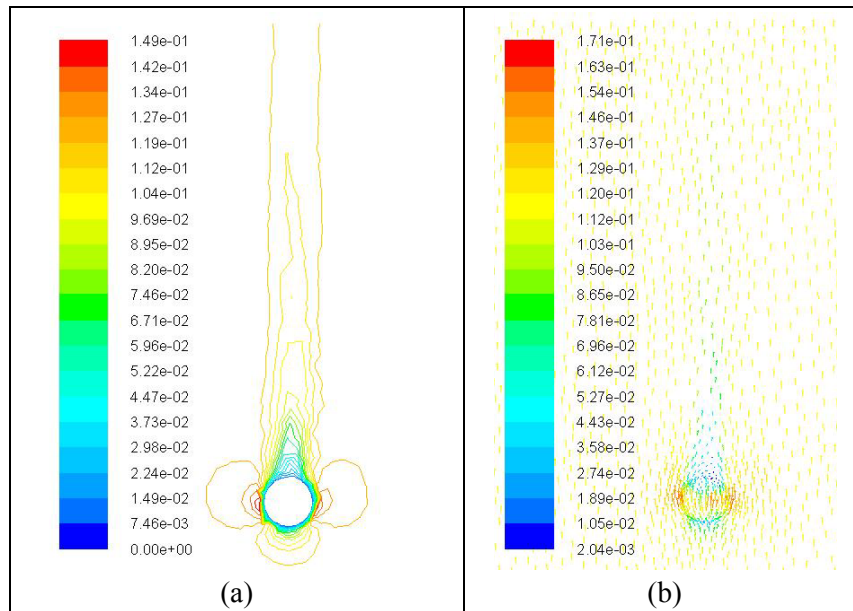

Figure 2:   Illustration of: (a) contour of velocity magnitude (m s^{-1}); and (b) velocity vector for the case of fluid inlet velocity of 0.117 m s^{-1} and the particle temperature of 318K and operating pressure of 3000 psi.

3.3   Heat Transfer

The result of heat transfer is presented in Figure 3 as the temperature profile of the surrounded carbon dioxide and the local heat flux on the particle surface. It is noticed that higher temperature region is distributed along the ring eddy flow at downstream of the sphere. It proves that the recirculation of the flow above the sphere enhances the heat transfer. The lowest heat flux occurred at the stagnation point where the flow velocity is equal to zero while the highest heat transfer happens at the side of particle where the velocity is the highest. Higher heat flux is obtained when the particle is set to a higher temperature due to the larger driving force of transfer. The higher temperature region decreases significantly as the pressure increase.
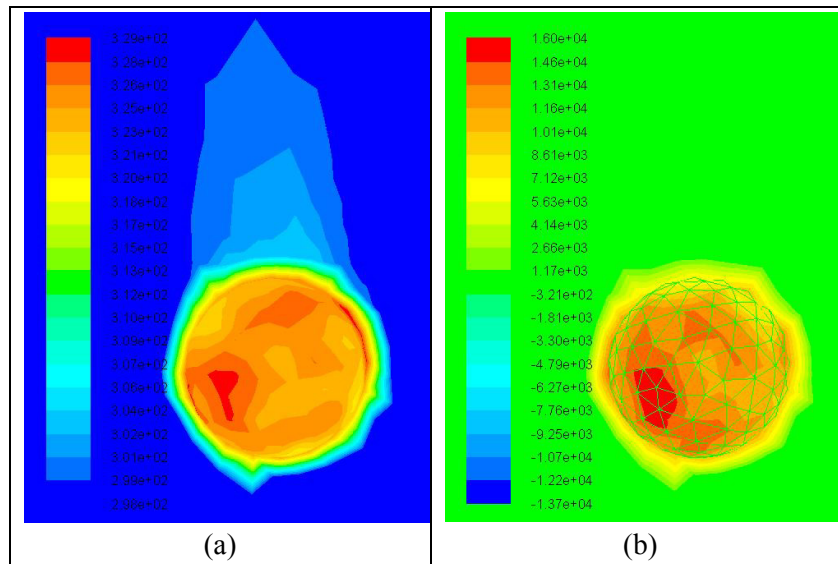
Figure 3: Illustration of: (a) the temperature profile of the surrounded CO_2 of a heated particle (K); and (b) the local heat flux value on the particle surface (W m^{-2}) for the inlet velocity of 0.117 m s^{-1}, particle surface temperature of 328K and operating pressure of 3000 psi.

3.4   Validation

The values of drag coefficient obtained from the simulations were compared with the literature correlations. The results are shown in Figure 4a. Overall, the drag coefficients predicted by CFD are lower than those determined from literature correlations. Higher agreement is achieved with the correlation of Feng[11] with the highest difference no greater than 5%. Although the values are somewhat different with A. Haider correlation and Clift correlation, the response towards the changes of Reynolds number is the similar, where the drag coefficient decrease with increase of Re. The values show some fluctuation at the range of Reynolds number 1000–1500. A transition flow model should be used in this range of Reynolds number in order to improve the results.
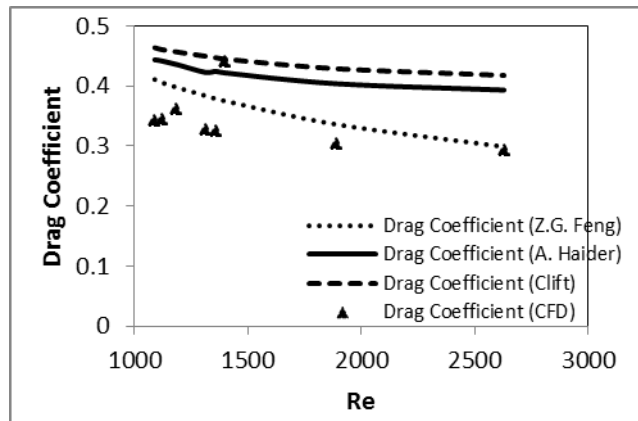
(a)
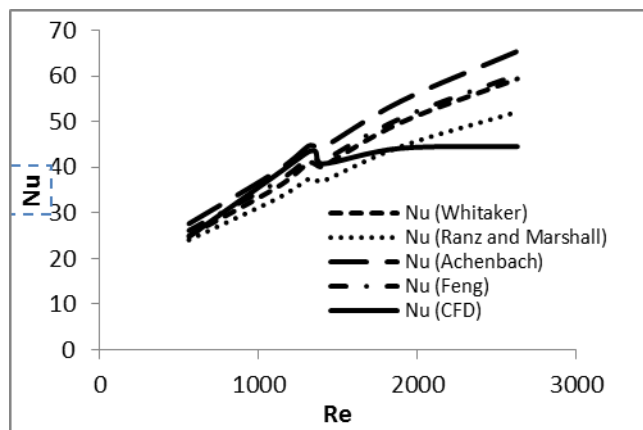
(b)

Figure 4: Illustration of: (a) comparison of drag coefficient between CFD computed value and correlation of experiment result; and (b) comparison of Nu between CFD computed value and the literature numerical correlation.

The results of Nu are validated against the literature correlations and the comparison is shown in Figure 4(b). The results for Reynolds number < 1500 show excellent agreement with all of the literature correlations. Yet, the value seems to be under predicted for higher Reynolds number. Number of mesh near the particle surface should be increased during the simulation of higher Reynolds number case in order to capture the details of the heat transfer and obtain and precise results.

4.   CONCLUSION

The flow behaviour of a supercritical fluid flowing through the spherical particle in vertical direction was examined and the heat transfer phenomenon has been studied. The fluid velocity is found to bring to rest at the forward stagnation point of the particle and increases with the increase of stagnation angle. The ring eddy flow occurring after the separation point has enhanced the heat transfer process. The lowest heat flux occurs at the stagnation point where the flow velocity is equal to zero, while the highest heat transfer happens at the side of particle where the velocity is the highest. The flow pattern and heat transfer results are compared with the literature correlations. The drag coefficients are found to have the same trend towards the changes of Reynolds number as the prediction of the literature correlations, even though the overall values are lower than those estimated by the correlations. The Nu for Re < 1500 shows an excellent agreement with all of the literature correlations.

5.   ACKNOWLEDGEMENT

6.   REFERENCES

1.   Srinivasan, K. (2009). Black pepper (*Piper nigrum*) and its bioactive compound, piperine. In Aggarwal, B. B. (Ed). *Molecular targets and therapeutic uses of spices: Modern uses for ancient medicine*. Singapore: World Scientific Publishing Co., 25–64.
2.   Bruner, G (2005). Supercritical fluids: Technology and application to food processing. *J. Food Eng.*, 1–2, 21–33.
3.   Reverchon, E. et al. (1999). Supercritical fractional extraction of fennel seed oil and essential oil: Experiments and mathematical modeling. *Ind. Eng. Chem. Res.*, 3069–3075.
4.   Salgın, U., Döker, O. & Calimli, A. (2006). Extraction of sunflower oil with supercritical CO_2 . *J. Supercrit. Fluids*, 38, 326–331.
5.   Meghwal, M. & Goswami, T. K. (2011). Thermal properties of black pepper and its volatile oil. *Int. J. Adv. Biotechnol. Res.*, 2(3), 334–344.
6.   Yaws, C. L. (1996). *Handbook of thermodynamic diagrams vol. 1: Organic ccompounds C1 to C4*. Houston: Gulf Publishing Company.
7.   Fenghour, A. & Wakeham, W. A. (1998). The viscosity of carbon dioxide. *J. Phys. Chem. Ref. Data*, 27, 31–44.

8. Ranz, W. E. & Marshall, W. R. (1952). Evaporation from drops. *Chem. Eng. Prog.*, 48, 141–146.

9. Whitaker, S. (1972). Forced convection heat transfer correlations for flow in pipes, past flat plates, single cylinders, single spheres and for flow in packed beds and tube bundles. *AIChE J.*, 18(2), 361–371.

10. Achenbach, E. (1995). Heat and flow characteristics of packed beds. *Exp. Therm. Fluid Sci.*, 1, 17–27.

11. Feng, Z. G. & Michealides, E. E. (2001). Heat and mass transfer coefficients of viscous spheres. *Int. J. Heat Mass Trans.*, 44, 4445–4454.

12. Clift, R., Grace, J. R. & Weber, M. E. (1987). *Bubbles drops and particles*. New York: Academic Press.

13. Haider, A. & Levenspiel, O. (1989). Drag coefficient and terminal velocity of spherical and nonspherical particles. *Power Technol.*, 58, 63–70.

14. Dixon, A. G. et al. (2011). Systematic mesh development for 3D CFD simulation of fixed beds: Single sphere study. *Comp. Chem. Eng.*, 35, 1171–1185.